

Regioselectivity for Condensation Reactions of Quinonoid Models of Tryptophan Tryptophylquinone: A Density Functional Theory Study

Jian-Wei Zou, Ji-Ming Liang, and Chin-Hui Yu*

Department of Chemistry, National Tsing Hua University, Hsinchu 300, Taiwan

chyu@oxygen.chem.nthu.edu.tw

Received December 3, 2002

The model compounds of tryptophan tryptophylquinone (TTQ), *o*-benzoquinone (OBQ), 3-methyl-6,7-dihydro-1*H*-6,7-indoledione (MIQ), and 3-methyl-4-(3-methyl-1*H*-2-indolyl)-6,7-dihydro-1*H*-6,7-indoledione (IIQ), all of which are characteristic of *o*-quinone groups, have been studied with density functional theory. The dihedral angle of the two indole rings (χ) of IIQ is calculated to be 49.6° for the global minimum. Another local minimum, 0.74 kcal/mol higher in energy, with a χ value of 123.5° is also fully optimized. The transition state connecting the two minima, with a χ value of 97.9°, has been located and the rotation barrier is 1.71 kcal/mol. A scan of the potential energy surface along this dihedral angle showed that the difference of the total energy was within 1.0 kcal/mol at a range of the dihedral angle from 30° to 75°. Hence, IIQ is flexible for the rotation of inter-indole rings. The origin of regioselectivity for the condensation reactions of the models MIQ and IIQ with NH₃ has been elucidated. It is shown that the energy difference between the two different types of carbinolamine intermediates (ΔE) and their corresponding transition structures (ΔE^\ddagger) should be responsible for the regioselectivity. To assess the effect of the fused ring on regioselectivity of the condensation reaction, a series of models were designed. A good linear correlation has been found between the energy difference of the two different carbinolamine intermediates (ΔE) and that of the corresponding transition states (ΔE^\ddagger), suggesting that the factors that stabilize the carbinolamine intermediate also favor the stability of the corresponding transition structure. The pair, 6-amino-6-hydroxy-8-methyl-6*H*-quinolin-5-one and 5-amino-5-hydroxy-8-methyl-5*H*-quinolin-6-one (**7/8**), deviates from the correlation and represents some anomalous behavior, which may be due to their structural particularity. It also has been shown that the tricyclic models, which consist of OBQ and two fused heterocyclic rings, represent more regioselectivity in contrast to the bicyclic systems. Moreover, the fused electron-donating pyrrole and the fused electron-withdrawing pyridine or pyrimidine show a somewhat synergistic effect on each other via the medial OBQ molecule. The barrier of the condensation reaction for pyrrolo[2,3-*f*]quinoline-4,5-dione is calculated to be ca. 22 kcal/mol. This is lower than that for MIQ (ca. 33 kcal/mol) and IIQ (ca. 32 kcal/mol) by as much as 10.0 kcal/mol, explaining reasonably the larger catalytic effect of pyrroloquinolinequinone (PQQ) relative to TTQ.

Introduction

For the oxidative deamination of primary amines (RR'CHNH₂) to ketones (RR'C=O), the most efficient reagent is 3,5-di-*tert*-butyl-1,2-benzoquinone (DTBQ), Corey's reagent,¹ which is *biomimetic* and a useful synthetic tool under adequate conditions. Corey's reagent, however, does not appear to be effective for the conversion of primary amines (RCH₂NH₂) to aldehydes (RCHO), since benzoxazolines and benzoxazoles are formed by side reactions of the desired Schiff bases.² Recently, a number of synthetic model studies for cofactors of quinoproteins have been investigated to understand the specificity of chemical structure of the cofactors and the mechanism

of catalytic reactions. For example, there are cofactors tryptophan tryptophylquinone (TTQ),³ pyrroloquinolinequinone (PQQ),⁴ and 2,4,5-trihydroxyphenylalanine quinone (topa quinone, TPQ).⁵ The model compounds^{6–9} designed according to the three cofactors are able to

(1) Klein, R. F. X.; Bargas, L. M.; Horak, V. *J. Org. Chem.* **1988**, *53*, 5994.

(2) Corey, E. J.; Achiwa, K. J. *J. Am. Chem. Soc.* **1969**, *91*, 1429.

(3) McIntire, W. S.; Wemmer, D. E.; Chistoserdov, A.; Lidstrom, M. E. *Science* **1991**, *252*, 817.

(4) (a) Salisbury, S. A.; Forrest, J. S.; Cruse, W. B. T.; Kennard, O. *Nature* **1979**, *280*, 843. (b) Westerling, J.; Frank, J.; Duine, J. A. *Biochem. Biophys. Res. Commun.* **1979**, *87*, 719.

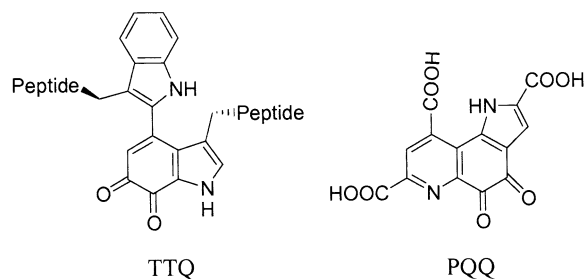
(5) Janes, S. M.; Mu, D.; Wemmer, D.; Smith, A. J.; Kaur, S.; Maltby, D.; Burlingame, A. L.; Klinman, J. P. *Science* **1990**, *248*, 981.

(6) Itoh, S.; Takada, N.; Haranou, S.; Ando, T.; Komatsu, M.; Ohshiro, Y.; Fukuzumi, S. *J. Org. Chem.* **1996**, *61*, 8967.

(7) (a) Itoh, S.; Mure, M.; Ogino, M.; Ohshiro, Y. *J. Org. Chem.* **1991**, *56*, 6857. (b) Itoh, S.; Takada, N.; Ando, T.; Haranou, S.; Huang, X.; Uenoyama, Y.; Ohshiro, Y.; Komatsu, M.; Fukuzumi, S. *J. Org. Chem.* **1997**, *62*, 5898. (c) Itoh, S.; Taniguchi, M.; Takada, N.; Nagatomo, S.; Kitagawa, T.; Fukuzumi, S. *J. Am. Chem. Soc.* **2000**, *122*, 12087.

(8) Lee, Y.; Sayre, L. M. *J. Am. Chem. Soc.* **1995**, *117*, 3096. (b) Mure, M.; Klinman, J. P. *J. Am. Chem. Soc.* **1995**, *117*, 8698.

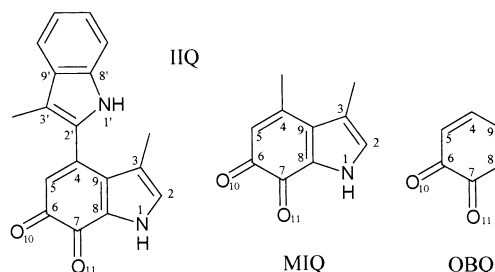
SCHEME 1



efficiently catalyze the oxidative deamination of $\text{PhCH}_2\text{-NH}_2$ to PhCHO in contrast to DTBQ. An investigation of structural specificity and catalytic mechanism would be valuable because further and useful information would help the development of an even more efficient reagent.

Cofactor TTQ, as shown in Scheme 1, is the redox-active prosthetic group in a number of enzymes,^{3,10–15} such as methylamine dehydrogenase (MADH, EC 1.4.99.3)^{12,16–18} and aromatic amine dehydrogenase (AADH).¹⁹ Since TTQ is tightly associated in the enzyme matrix through amide linkages, it is difficult to isolate the prosthetic group and to perform mechanistic studies of the redox reactions. Nevertheless, a transamination mechanism has been proposed for enzymatic amine oxidation.^{3,20–23} The reaction is initiated with a nucleophilic attack by the amino group of the primary amine at the C-6 position of quinone carbonyls, i.e. a condensation reaction. Subsequently, rearrangement and hydrolysis are followed by electron transfer; in the process, MADH sequentially transfers two electrons to a c-type cytochrome^{24,25} via a mediating blue copper protein, amicyanin.^{26,27} The X-ray crystallographic investigation of MADHs reveals that the dihedral angle of $\text{C}_5\text{--C}_4\text{--C}_2\text{--}$

SCHEME 2



$\text{C}_3'\text{--}(\chi)$ of TTQ is about 42° .^{10,16} The analysis of orientation-restricted electron nuclear double resonance (ENDOR) spectra shows that the two indole ring planes rotate freely along the axis of their covalent linkage within a range of dihedral angle of $48 \pm 11^\circ$.²⁸ Some experimental data^{10,11,28} suggest that the main chain around the cofactor does not change the conformation significantly during the direct reduction of the oxidized TTQ to its semiquinone states. In other words, internal strain energy is negligible between the cofactor and the polypeptide backbone that bridges to the cofactor in both the oxidized and the semiquinone states of TTQ in MADH.

Recently, the successful synthesis of a model compound of TTQ, 3-methyl-4-(3-methyl-1*H*-2-indolyl)-6,7-dihydro-1*H*-6,7-indoledione (IIQ, Scheme 2), provided an insight into the structure and properties of the TTQ cofactor in the active site of MADH.^{29,30} The electronic and resonance Raman spectra of IIQ³⁰ are very similar to those of the TTQ cofactor of native enzymes. IIQ has exactly the same ring skeleton of TTQ, except that the two polypeptide chains at 3- and 3'-positions are replaced by simple methyl groups. The downshifted vibrational frequencies of resonance Raman of TTQ provide the first direct evidence that a monovalent cation occupying a cation binding site is interacting with the C-6 carbonyl oxygen of the TTQ cofactor.³¹ Molecular orbital calculations of IIQ by the semiempirical AM1 method³² indicate that the dihedral angle χ is 46.9° in the optimized structure of the IIQ compound and the difference in the heat of formation is less than 1.0 kcal/mol at a dihedral angle of ca. $30\text{--}130^\circ$ with a local maximum of ca. 0.8 kcal/mol at ca. 100°C .³⁰ Furthermore, IIQ also acts as an efficient reagent for accelerating the oxidation of benzylamine in nonenzymatic systems.^{6,29} For the condensation reaction, the iminoquinone-type adducts of several primary amines and IIQ were isolated and it was found that amines were bounded at C-6 of IIQ from the observed NOE,⁶ in agreement with the proposed mechanism of the TTQ cofactor. Thermodynamic stability of the carbinolamine intermediate was proposed by these authors⁶ to be responsible for the regioselectivity because they found that the C-6 carbinolamine intermediate of cyclopropylamine and IIQ is more stable than the C-7 carbinolamine intermediate by 2.9 kcal/mol at the PM3 calculations.³³

(9) (a) Rinaldi, A. C.; Rescigno, A.; Rinaldi, A.; Sanjust E. *Bioorg. Chem.* **1999**, *27*, 253. (b) Largeron, M.; Fleury, M.-B. *J. Org. Chem.* **2000**, *65*, 8874.

(10) Chen, L.; Mathews, F. S.; Davidson, V. L.; Huizinga, E. G.; Vellieux, F. M. D.; Duine, J. A.; Hol, W. G. J. *FEBS Lett.* **1991**, *287*, 163.

(11) Chen, L.; Mathews, F. S.; Davidson, V. L.; Huizinga, E. G.; Vellieux, F. M. D.; Hol, W. G. J. *Proteins* **1992**, *14*, 288.

(12) Davidson, V. L. In *Principles and Applications of Quinoproteins*; Davidson, V. L., Ed.; Marcel Dekker: New York, 1993; p 73.

(13) McIntire, W. S. *Methods Enzymol.* **1995**, *258*, 149.

(14) Itoh, S.; Ohshiro, Y. *Methods Enzymol.* **1995**, *258*, 164.

(15) Davidson, V. L.; Brooks, H. B.; Graichen, M. E.; Jones, L. H.; Hyun, Y. L. *Methods Enzymol.* **1995**, *258*, 176.

(16) Sun, D. P.; Jones, L. H.; Mathews, F. S.; Davidson, V. L. *Protein Eng.* **2001**, *14*, 675.

(17) Wang, Y. T.; Sun, D. P.; Davidson, V. L. *J. Biol. Chem.* **2002**, *277*, 4119.

(18) Chen, L.; Durley, R. C. E.; Mathews, F. S.; Davidson, V. L. *Science* **1994**, *264*, 86.

(19) Govindaraj, S.; Eisenstein, E.; Jones, L. H.; Sanders-Loehr, J.; Chistoserdov, A. Y.; Davidson, V. L.; Edwards, S. L. *J. Bacteriol.* **1994**, *176*, 2922.

(20) Kano, K.; Nakagawa, M.; Takagi, K.; Ikeda, T. *J. Chem. Soc., Perkin Trans. 2* **1997**, 1111.

(21) Davidson, V. L.; Jones, L. H.; Graichen, M. E. *Biochemistry* **1992**, *31*, 3385.

(22) Lee, Y.; Sayre, L. M. *J. Am. Chem. Soc.* **1995**, *117*, 11823.

(23) Brooks, H. B.; Jones, L. H.; Davidson, V. L. *Biochemistry* **1993**, *32*, 2725.

(24) Husain, M.; Davidson, V. L. *J. Biol. Chem.* **1986**, *261*, 8577.

(25) Gray, K. A.; Knaff, D. B.; Husain, M.; Davidson, V. L. *FEBS Lett.* **1986**, *207*, 239.

(26) Sun, D. P.; Davidson, V. L. *Biochemistry* **2001**, *40*, 12285.

(27) Chen, L.; Durley, R.; Poliks, B. J.; Hamada, K.; Chen, Z.; Mathews, F. S.; Davidson, V. L.; Satow, Y.; Huizinga, E.; Vellieux, F. M. D.; Hol, W. G. J. *Biochemistry* **1992**, *31*, 4959.

(28) Warncke, K.; Brooks, H. B.; Lee, H.; McCracken, J.; Davidson, V. L.; Babcock, G. T. *J. Am. Chem. Soc.* **1995**, *117*, 10063.

(29) Ohshiro, Y.; Itoh, S. *Pure Appl. Chem.* **1994**, *66*, 753.

(30) Itoh, S.; Ogino, M.; Haranou, S.; Terasaka, T.; Ando, T.; Komatsu, M.; Ohshiro, Y.; Fukuzumi, S.; Kano, K.; Takagi, K.; Ikeda, T. *J. Am. Chem. Soc.* **1995**, *117*, 1485.

(31) Moenne-Loccoz, P.; Nakamura, N.; Itoh, S.; Fukuzumi, S.; Gorren, A. C. F.; Duine, J. A.; Sanders-Loehr, J. *Biochemistry* **1996**, *35*, 4713.

(32) Dewar, M. J. S.; Zebisch, E. G.; Healy, E. F.; Stewart, J. J. P. *J. Am. Chem. Soc.* **1985**, *107*, 3902.

An examination of the structure of IIQ and the carbinolamine intermediates of IIQ and primary amines reveals that the fused pyrrole ring, i.e. 3-methyl-6,7-dihydro-1*H*-6,7-indoledione (MIQ), shown in Scheme 2, plays a vital role in the reactions. It is also found that PQQ (Scheme 1) features an even larger catalytic effect than TTQ for similar reactions.^{7a} As the reaction center of PQQ is an *o*-benzoquinone fused with two rings, in addition to the exact influence of the electron-withdrawing effect of the fused pyridine ring in PQQ, the multiring system seems to have stronger effect on the reaction.

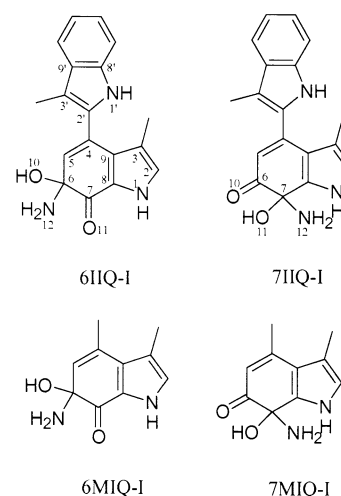
The aim of this paper is, on one hand, to use reliable theoretical simulations to provide thorough information on the molecular structure of IIQ and its fragments, namely MIQ and *o*-benzoquinone (OBQ, Scheme 2). On the other hand, a more important goal is to explore the origin of the regioselectivity and the structure–regioselectivity relationship of quinonoid compounds with primary amines. Thus, a series of miscellaneous model compounds consisting of different nitrogen-containing heterocyclic rings and OBQ, mostly derived from the frameworks of TTQ and PQQ, were investigated. These model compounds comprised three groups of isosteres, and included different position and number of the nitrogen atom in the ring attached to the quinonoid ring, a different size of the attached ring, and different numbers of fused rings; details will be described in the next section.

Theoretical Models and Computational Details

Molecular structures of IIQ and its fragments, MIQ and OBQ, were thoroughly examined computationally. The potential energy surface (PES) as a function of the dihedral angle between the indole ring and indole–quinone ring, i.e. the dihedral angle C₅–C₄–C₂–C₃, χ , as marked in Scheme 2, was then followed. The two minima and the transition state were fully optimized; other points were constraint optimization with χ being fixed. This PES could provide information on the TTQ conformation and helped in understanding the nature of the freely conformational change of IIQ. Hence, it was deemed worthy of study at a higher theoretical level in addition to previous MM and semiempirical data.^{28,30} Vibrational analyses were also performed at the same level of theory. Comparisons among IIQ and its fragments as well as between experimental and theoretical data were carried out to further explore the properties of model compounds of TTQ.

The condensation reaction is the first step of the transamination mechanism of TTQ in the oxidative deamination of primary amines to the corresponding aldehydes. This reaction involves two consecutive processes: first, a nucleophilic attack by the amine nitrogen on one of the quinone carbonyls resulting in a carbinolamine intermediate, and second, a loss of a water molecule to form an iminoquinone. It has been shown by Itoh et al.⁶ that the additive step of amine to quinone is rate-determining. This step is therefore thought to be crucial for the regioselectivity. To explore the origin of regioselectivity and the effect of the substituted indole ring upon the regioselectivity, the carbinolamine intermediates of the condensation reaction of MIQ and NH₃ (6MIQ-I and 7MIQ-I), IIQ and NH₃ (6IIQ-I and 7IIQ-I) (see Scheme 3), as well as their corresponding transition states were studied. Natural population analysis (NPA) was applied to probe properties related to electron density. Some calculations with the MP2 method were performed to check the convergence.

SCHEME 3



The 6 π -electron aromatic five- and six-membered rings possess the advantage of few side reactions and the delocalization of π electrons can accelerate the electron-transfer process. Thus, we designed a series of carbinolamine intermediates produced from condensation reactions of ammonia and heterocyclic quinonoid compounds involving five-membered or six-membered fused rings. The bicyclic carbinolamine intermediates of the quinonoid compounds with five-membered fused pyrrole and imidazole rings (**1**–**4**) and six-membered fused pyridine and pyrimidine rings (**5**–**10**) are shown in Scheme 4. Another important factor investigated was the adductive effect that results from OBQ being simultaneously bounded with a five-membered and a six-membered ring. The tricyclic models consisting of OBQ, pyrrole, and pyridine or pyrimidine (**11**–**16**) are shown in Scheme 5. The goal of studying these model compounds by theoretical calculations is to provide knowledge into how the fused heterocyclic rings affect the regioselectivity and what fused rings would have higher regioselectivity.

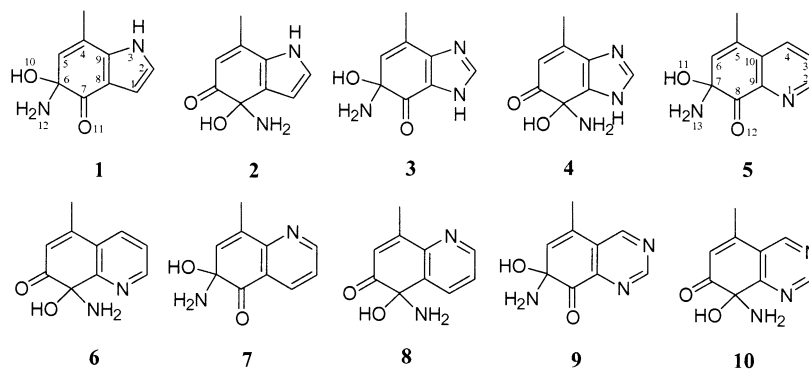
The hybrid density functional method, B3LYP,^{34,35} with the D95(d,p)³⁶ basis set was chosen because of its agreeable record in determining molecular structures, relative energies, and vibrational frequencies.^{37–39} A basis set with diffuse functions, however, usually has significant influence on the relative energies of hydrogen-bonded systems.⁴⁰ Hence, the model compounds, 6MIQ-I, 7MIQ-I, and **1**–**16**, as well as their corresponding transition structures were fully optimized by both B3LYP/D95(d,p) and B3LYP/D95++(d,p) to yield better comparison of the relative energy. The effect of the augmented diffuse functions was evaluated.

The geometry optimization and vibrational frequencies were calculated with Gaussian 94⁴¹ on IBM/390 and SGI Power-

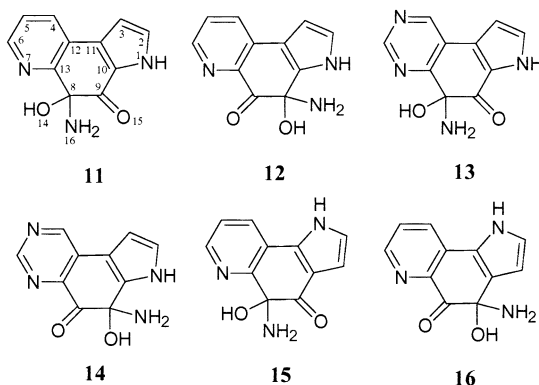
(33) (a) Stewart, J. J. P. *J. Comput. Chem.* **1989**, *10*, 209. (b) Stewart, J. J. P. *J. Comput. Chem.* **1989**, *10*, 221.

(34) Lee, C.; Yang, W.; Parr, R. G. *Phys. Rev. B* **1988**, *37*, 785.
 (35) Becke, A. D. *J. Chem. Phys.* **1993**, *98*, 5648.
 (36) (a) Huzinaga, S. *J. Chem. Phys.* **1965**, *42*, 1293. (b) Dunning, T. H. *J. Chem. Phys.* **1970**, *53*, 2823.
 (37) Banks, H. D.; White, W. E. *J. Org. Chem.* **2001**, *66*, 5981.
 (38) Castejon, H.; Wiberg, K. B.; Sklenak, S.; Hinz, W. *J. Am. Chem. Soc.* **2001**, *123*, 6092.
 (39) Ilieva, S.; Hadjieva, B.; Galabov, B. *J. Org. Chem.* **2002**, *67*, 6210.
 (40) Csonka, G. I.; Elias, K.; Csizmadia, I. G. *Chem. Phys. Lett.* **1996**, *257*, 49.
 (41) Frisch, M. J.; Trucks, G. W.; Schlegel, H. B.; Gill, P. M. W.; Johnson, B. G.; Robb, M. A.; Cheeseman, J. R.; Keith, T.; Petersson, G. A.; Montgomery, J. A.; Raghavachari, K.; Al-Laham, M. A.; Zakrzewski, V. G.; Ortiz, J. V.; Foresman, J. B.; Cioslowski, J.; Stefanov, B. B.; Nanayakkara, A.; Challacombe, M.; Peng, C. Y.; Ayala, P. Y.; Chen, W.; Wong, M. W.; Andres, J. L.; Replogle, E. S.; Gomperts, R.; Martin, R. L.; Fox, D. J.; Binkley, J. S.; Defrees, D. J.; Baker, J.; Stewart, J. P.; Head-Gordon, M.; Gonzalez, C.; Pople, J. A. *Gaussian 94*, revision C.2; Gaussian, Inc.: Pittsburgh, PA, 1995.

SCHEME 4



SCHEME 5



Challenge XL workstations, and with Gaussian 98⁴² compiled on PC-Linux systems.⁴³ Default Berny analytical gradient optimization method and threshold values of converged criteria were used in the optimization. For convenience, we utilized n-TS to denote the transition state corresponding to the carbinolamine intermediate, n. All transition structures whose schematic diagrams are shown in Figure 1 were characterized by frequency calculations to ensure that they had one and only one imaginary frequency.

Results and Discussion

Geometries of Model Compounds Related to IIQ.

Some structural parameters of the optimized geometry of OBQ, MIQ, and IIQ are listed in Table S1 along with available experimental data.¹⁰ This table is provided as Supporting Information. It has been shown that the similarity between IIQ and the TTQ cofactor in its native protein is remarkable. The most notable differences occur around the polar quinone group. This fact is readily understood since there are water molecules incorporated

in the *o*-quinone groups of TTQ cofactor in the MADH crystal structure.^{10,44,45} Hence, the drastic deviations of the *o*-quinone groups between the theoretical data and experimental data may be attributed to the distorted structure in X-ray crystallographic analyses.

The C–C bond of adjacent carbonyl groups, C₆–C₇, of the OBQ, MIQ, and IIQ is ~1.56 Å, slightly longer than an ordinary C–C single bond due to the strong repulsions of π bonds and lone pairs of carbonyl groups. This results in the destruction of aromaticity of quinonoid structures and may have changed the reactivity of quinonoid compounds. Moreover, IIQ features the shortest C₆–C₇ bond due to a slight reduction of the electronic repulsions of carbonyl groups caused by the delocalization between the indole ring and the indole–quinone ring. NPA indeed shows that the natural charges of C-6 and C-7 in IIQ are 0.486 and 0.468 au, respectively, lower than those of corresponding values in MIQ, 0.494 and 0.469 au, respectively. Unlike the exact planarity of the indole ring in MIQ, the indole ring and the indole–quinone ring in the IIQ moiety are slightly distorted, which can be ascribed to the strong repulsions between the indole–quinone ring and the indole ring. The lengths of the two C=O bonds of MIQ and IIQ are almost the same, but those of the two C=O bonds of OBQ slightly differ from those of MIQ and IIQ. This indicates that the directly fused pyrrole ring has a significant influence on the distribution of electron density of OBQ through the strong resonance effect. This argument has been further supported by NPA (see Supporting Information).

The C₄–C₉ bond of IIQ is the longest due to the repulsion between the indole ring and the indole–quinone ring. There is a certain degree of conjugation between the two indole rings, revealed by the short C–C bond, 1.468 Å, between the indole ring and the indole–quinone ring, the C₄–C_{2'} bond. The degree of conjugation varies according to the dihedral angle between the indole ring, C₅–C₄–C_{2'}–C_{3'} (χ). It is obvious that the weakest conjugation is approximately at the dihedral angle of

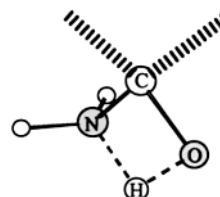


FIGURE 1. Schematic diagram of the structure of the transition state of the addition of amine to quinone.

(42) Frisch, M. J.; Trucks, G. W.; Schlegel, H. B.; Scuseria, G. E.; Robb, M. A.; Cheeseman, J. R.; Zakrzewski, V. G.; Montgomery, J. A., Jr.; Stratmann, R. E.; Burant, J. C.; Dapprich, S.; Millam, J. M.; Daniels, A. D.; Kudin, K. N.; Strain, M. C.; Farkas, O.; Tomasi, J.; Barone, V.; Cossi, M.; Cammi, R.; Mennucci, B.; Pomelli, C.; Adamo, C.; Clifford, S.; Ochterski, J.; Petersson, G. A.; Ayala, P. Y.; Cui, Q.; Morokuma, K.; Rega, N.; Salvador, P.; Dannenberg, J. J.; Malick, D. K.; Rabuck, A. D.; Raghavachari, K.; Foresman, J. B.; Cioslowski, J.; Ortiz, J. V.; Baboul, A. G.; Stefanov, B. B.; Liu, G.; Liashenko, A.; Piskorz, P.; Komaromi, I.; Gomperts, R.; Martin, R. L.; Fox, D. J.; Keith, T.; Al-Laham, M. A.; Peng, C. Y.; Nanayakkara, A.; Challacombe, M.; Gill, P. M. W.; Johnson, B.; Chen, W.; Wong, M. W.; Andres, J. L.; Gonzalez, C.; Head-Gordon, M.; Replogle, E. S.; Pople, J. A. *Gaussian 98*, revision A.11; Gaussian, Inc.: Pittsburgh, PA, 2001.

(43) Yu, J.-S. K.; Yu, C.-H. *J. Chem. Inf. Comput. Sci.* **2002**, *42*, 673.

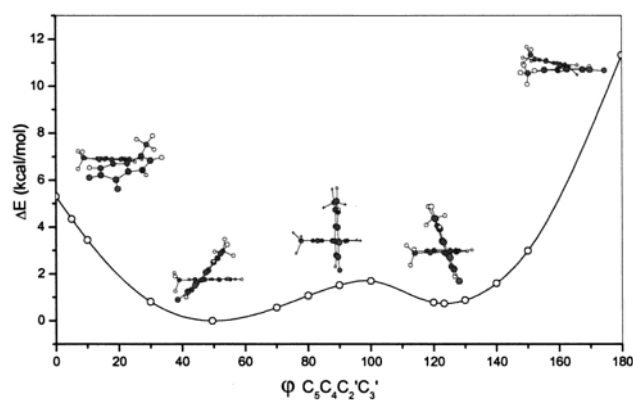


FIGURE 2. The potential energy surface of IIQ along the dihedral angle $\varphi_{C_5C_4C_2'C_3'}$.

90.0°. The dihedral angle of the global minimum of the ground state, however, is 49.6°. It indicates that the electronic effects, i.e. conjugation and repulsion, especially between methyl groups and the opposite hydrogen atoms, achieve a certain subtle balance. The calculated value of χ differs about 7.6° in comparison to that of the X-ray crystallographic investigation of MADH, which has been reported to be 42°,¹⁰ or about 2° and 7.7° differences for the two TTQ cofactors of MADH.^{44,45} The data show that the two indole rings of TTQ are highly flexible in the internal rotation over a wide range of χ .

The differences of structures and energies from the PES along the dihedral angle χ are listed in Table S2 in the Supporting Information. As clearly shown in Figure 2, there is another local minimum (IIQ'), which is fully optimized without any geometrical restriction, with a dihedral angle 123.5° and an energy 0.74 kcal/mol higher than the global minimum. The transition state (IIQ-TS) between the two local minima with a χ value of 97.9° has been located. The energy of IIQ-TS is 1.71 kcal/mol relative to the global minimum. In addition, the difference of the total energy of IIQ is within 1.0 kcal/mol at a region of dihedral angle from 30° to 75°. In fact, the indole ring and indole-quinone ring of IIQ itself can freely rotate around the C₄-C_{2'} bond from ca. 15° to ca. 150° where the energy varies within 2.0 kcal/mol at room temperature. Hence, the mobile region shown in the spectral data of orientation-restricted ENDOR²⁸ is primarily responsible for interactions between TTQ and nearby amino acids in the active site of MADH. The resonance effect of IIQ is strongest at $\chi = 0.0^\circ$ or 180° , as shown in the trend of the variation of the C₄-C₅ bond, the C₅-C₆ bond, and the C₆-C₇ bond. Even the most strongly affected bond lengths and bond angles only vary less than ca. 0.03 Å and ca. 3° during the course, respectively.

Harmonic Vibrational Frequencies. The calculated vibrational frequencies, scaled by a factor of 0.96,⁴⁶ of OBQ, MIQ, and IIQ are listed in Table S3 (Supporting Information). The peak positions of the resonance Raman (RR) spectra are a property of the ground electronic state

and the peak intensities are strongly dependent on the excited electronic states as well as on the ground state. Hence, RR spectra contain features which represent vibrational modes of the ground electronic state and are analogous to IR spectra.⁴⁷

The *o*-quinone groups are characteristic of high reactivity for condensation reactions. The frequency of the C=O stretch of IIQ, $\nu(C=O)$, is measured as 1638 cm⁻¹ in H₂O.³¹ This corresponds to the asymmetric stretching mode of C=O of 1683 cm⁻¹ by theoretical calculations. The small difference of 45 cm⁻¹ partially results from the carbonyl groups being sensitive to the solvent environment, i.e. polarization of the carbonyl groups by solvent molecules. Therefore, solvent polarization causes reduction of the frequencies of carbonyl groups of IIQ by means of partial dispersion of electron density of the carbonyl group. For OBQ, the frequencies of carbonyl groups, $\nu(C=O)$, are 1680 and 1658 cm⁻¹ in the IR spectra.⁴⁸ The two values compare well with the calculated values (1703 and 1679 cm⁻¹). The frequencies of the C=O stretch decrease in the sequence OBQ, MIQ, and IIQ owing to the partial reduction of π -electron density of carbonyl groups with the increasing electron delocalization. The frequencies of the C₄-C₅ stretch mode of IIQ, 1556 cm⁻¹, are the lowest among the three simulated TTQ models in Table S3 because the π -electron density of the C₄-C₅ bond delocalizes into the pyrrole ring of the substituted indole ring. The lower frequencies of the C₈-C₉ of IIQ, 1507 cm⁻¹, can be attributed to the delocalization of the π -electron into the whole fused pyrrole and part of the pyrrole ring of the substituted indole ring. In summary, IIQ possesses the lowest frequencies of all four modes analyzed due to the more profound delocalization of this larger molecule.

The Origin of Regioselectivity. In the enzymatic system, it has been shown that the amine attacks selectively to the C-6 quinonoid carbonyl carbon of TTQ cofactor in the initial phase of reaction. The regioselectivity was ascribed to the space restriction at the enzyme active site. There is enough space for substrate-binding only near the C-6 carbonyl group.¹⁰ However, this argument was challenged by recent studies of Itoh et al., who found that the regioselectivity also existed in the model system IIQ as well as MIQ without enzyme. They performed semiempirical molecular orbital calculations, using the PM3 method, and proposed that the regioselectivity may result from the difference in thermodynamic stability of the two carbinolamine intermediates.⁶ Although the explanation is plausible, the semiempirical PM3 method seems to be somewhat crude. Moreover, another important aspect that the regioselectivity of the condensation reaction may be controlled by kinetics has not been taken into consideration in their work. There is no evidence to allow one to exclude this possibility in advance. Thus, it is necessary to further investigate the origin of the regioselectivity at a higher computational level and with kinetic factors.

(44) Macdonald, A. L.; Trotter, J. *J. Chem. Soc., Perkin Trans.* **1973**, 476.

(45) The data are downloaded from the protein data bank (<http://www.rcsb.org/pdb>) with the ID number 2bbk.

(46) Wong, M. W. *Chem. Phys. Lett.* **1996**, 256, 391.

(47) (a) Garey, P. R.; Schneider, H. *Acc. Chem. Res.* **1978**, 11, 122. (b) Carey, P. R. *Biochemical Applications of Raman and Resonance Raman Spectroscopies*; Academic Press: New York, 1982.

(48) Berger, St.; Rieker, A. In *The chemistry of the quinonoid compounds, Part I*; Patai, S., Ed.; John Wiley & Sons: London, UK, 1974; p 193.

TABLE 1. Calculated Total Energies (in au) and Relative Energies (in kcal/mol) of Carbinolamine Intermediates, 6MIQ-I, 7MIQ-I, 6IIQ-I, 7IIQ-I, and 1–16, as Well as Their Corresponding Transition States

	E_{tot} (carbinolamine intermediate)		ΔE_i^a	E_{tot} (transition state)		$\Delta E_i^{\ddagger a}$
	B3LYP/D95 (d,p)	B3LYP/D95++(d,p)		B3LYP/D95 (d,p)	B3LYP/D95++(d,p)	
6MIQ-I	−648.34894	−648.36742		−648.28703	−648.30581	
7MIQ-I	−648.34766	−648.36542	0.80 (1.26)	−648.28429	−648.30196	1.72(2.42)
6IIQ-I	−1011.02145			−1010.95972		
7IIQ-I	−1011.01782		2.28	−1010.95444		3.31
1	−609.02452	−609.04236		−608.96237	−608.98056	
2	−609.02343	−609.04105	0.68 (0.82)	−608.96104	−608.97858	0.83(1.24)
3	−625.07790	−625.09605		−625.01630	−625.03475	
4	−625.07796	−625.09549	−0.04 (0.35)	−625.01482	−625.03232	0.93(1.53)
5	−647.12929	−647.14632		−647.06850	−647.08591	
6	−647.13846	−647.15584	−5.76 (−5.98)	−647.08299	−647.10020	−9.09(−8.97)
7	−647.13817	−647.15548		−647.07765	−647.09542	
8	−647.14163	−647.15880	−2.17(−2.08)	−647.07860	−647.09571	−0.60(−0.18)
9	−633.17102	−663.18811		−663.11051	−663.12813	
10	−663.18245	−663.20000	−7.17 (−7.47)	−663.12672	−663.14419	−10.17(−10.08)
11	−739.41870	−739.43816		−739.36287	−739.38288	
12	−739.40602	−739.42523	7.96 (8.12)	−739.34239	−739.36127	12.85 (13.56)
13	−755.46306	−755.48267		−755.40696	−755.42685	
14	−755.44797	−755.46699	9.47 (9.84)	−755.38435	−755.40368	14.19(14.54)
15	−739.41419	−739.43376		−739.35848	−739.37825	
16	−739.40347	−739.42254	6.73 (7.04)	−739.34212	−739.36139	10.27 (10.58)

^a The values at B3LYP/D95++(d,p) are given in parentheses.

The NPA at the B3LYP/D95(d,p) level for MIQ shows that the atomic charge at C-6 (0.494) is larger than that of C-7 (0.469). This suggests the nucleophilic attack at the C-6 position is preferred, contrary to previous analysis by the PM3 method.⁶ However, the nucleophilic atomic frontier electron density (f_r^N)^{49,50} at C-6 (0.102) is calculated to be very close to that at C-7 (0.106), revealing that the reactivity of these two positions is almost identical. Herein we used a more efficient quantity, f_r^N , rather than the coefficient of LUMO that was used in Itoh et al.'s study⁶ to describe the reactivity of different atoms in the same molecule. Further calculations at a higher level MP2/6-311G(d,p) showed that the difference of atomic charges at these two carbons becomes smaller, while the values of f_r^N still slightly favor the nucleophilic attack at the C-7 position, cf. atomic charge = 0.559 (C-6), 0.553 (C-7), and f_r^N = 0.066 (C-6), 0.074 (C-7). Thus, it is difficult to evaluate the origin of the regioselectivity of the model compound by solely utilizing the electronic populations of the two quinonoid carbons.

In energy aspects, two factors may have given rise to regioselectivity. One is the difference in the thermodynamic stability of the C-6 and C-7 carbinolamine intermediates, and the other is the difference in the barrier of the two condensation reactions. If the dipole–dipole complex is neglected,^{37,51,52} the latter is, in fact, the energy difference between the transition state of C-6 condensa-

tion and that of C-7 condensation. The total energy of 6MIQ-I is calculated to be lower than that of 7MIQ-I by 0.80 kcal/mol at the B3LYP/D95(d,p) level, but lowered by 1.26 kcal/mol at the B3LYP/D95++(d,p) level (see Table 1). The incorporation of zero-point energy (ZPE) into the calculation has little effect on the relative energy: 0.66 kcal/mol at the B3LYP/D95(d,p) level. For stability of 6MIQ-I, the major contribution may have resulted from the smaller distortion, 4.9°, from planarity of the indole–quinone ring, in contrast to that of 7MIQ-I being 15.0°. For IIQ, the difference in energy between the two types of carbinolamine intermediates is predicted to be 2.28 kcal/mol at the B3LYP/D95(d,p) level. In addition, a comparison of the transition states for MIQ and IIQ systems shows that the energy of 6MIQ-I-TS is lower than that of 7MIQ-I-TS by 1.72 kcal/mol at the B3LYP/D95(d,p) level and 2.42 kcal/mol at the B3LYP/D95++(d,p) level, while the energy of 6IIQ-I-TS is lower than that of 7IIQ-I-TS by 3.31 kcal/mol at the B3LYP/D95(d,p) level. These results indicate clearly that both thermodynamics and kinetics of the condensation reaction favor the nucleophilic attack of amine at the C-6 position, in agreement with the experimental observation. On the other hand, the indole ring of IIQ can promote greater selectivity at C-6 compared to MIQ. Furthermore, it has been found that the absolute barriers for the condensation reactions of MIQ and IIQ with NH₃ are 32.70 and 31.64 kcal/mol at the B3LYP/D95(d,p) level, respectively. The condensation of IIQ has a lower barrier, indicating the substituted indole ring can also slightly accelerate the reaction.

Structure–Regioselectivity Relationship. To explore the effect of the fused pyrrole ring on the regioselectivity of the condensation reaction, a series of carbinolamine 1–16 were designed. The calculated energies of these compounds and those of their corresponding transition states are listed in Table 1, where the energy differences between the pair of carbinolamine intermediates of the same model system are listed as ΔE_i and the energy differences between the pair of transition states

(49) Fukui, K. *Theory of Orientation and Stereoselection*; Springer-Verlag: New York, 1975; p 34.

(50) Karelson, M.; Lobanov, V. S.; Katritzky, A. R. *Chem. Rev.* **1996**, *96*, 1027.

(51) (a) Castejon, H.; Wiberg, K. B. *J. Am. Chem. Soc.* **1999**, *121*, 2139. (b) Webb, S. P.; Gordon, M. S. *J. Phys. Chem. A* **1999**, *103*, 1265. (c) Hori, K.; Abboud, J.-L. M.; Lim, C.; Fujio, M.; Tsuno, Y. *J. Org. Chem.* **1998**, *63*, 4228.

(52) Dipole–dipole complexes are generally not taken into account in the computational studies of chemical reactions. In a few cases,^{51a,b} the dipole–dipole complexes are obtained and are found to lie slightly below the energy of the reactants. In the present work, optimizations of the dipole–dipole complexes lead actually to the hydrogen-bonded complexes. Therefore, the dipole–dipole complexes are neglected and the activation energies are calculated as the difference between the transition state energy and the sum of the energies of the reactants.

are listed as ΔE_i^\ddagger . The geometries of these carbinolamine intermediates and corresponding transition states are provided as Supporting Information.

As clearly revealed in the data, the position and numbers of nitrogen atoms of a fused ring influence greatly the changes of both ΔE_i and ΔE_i^\ddagger , where $\Delta E_i = E_{n+1} - E_n$ and $\Delta E_i^\ddagger = E_{n+1}^\ddagger - E_n^\ddagger$ for odd n , due to the variation between the electron-donating and electron-withdrawing nature of a fused ring. Especially, the quinonoid compounds with six-membered fused rings **5–10** favor the nucleophilic attack on the adjacent carbonyl carbon position more than those with five-membered fused rings, namely **1–4**. The drastic change of the regioselectivity between the five-membered fused rings and six-membered fused rings can be primarily ascribed to the strong resonance effect and smaller ring strain of the six-numbered fused rings. It is shown in the difference of the distorted degree from planarity of the molecular skeleton, revealed by the degree of change of the dihedral angle $C_6-C_7-C_8-C_9$ and the dihedral angle $C_7-C_8-C_9-C_{10}$, except for the case of 6-amino-6-hydroxy-8-methyl-6*H*-quinolin-5-one (**7**) and 5-amino-5-hydroxy-8-methyl-5*H*-quinolin-6-one (**8**). In general, the better a carbinolamine intermediate maintains planarity, the more a carbinolamine intermediate is thermodynamically stable.

Interestingly, it has been found that the energy difference between the two different carbinolamine intermediates (ΔE) correlates well with the energy difference between the corresponding transition states (ΔE^\ddagger) at both B3LYP/D95(d,p) and B3LYP/D95++(d,p) levels, as shown in eqs 1 and 2, implying that the factors stabilizing the carbinolamine intermediate also facilitate the stability of the corresponding transition structure.

$$\text{B3LYP/D95 (d,p): } \Delta E^\ddagger = 1.4799\Delta E + 0.5326 \\ (n = 10, r = 0.994, \text{sd} = 0.94) \quad (1)$$

$$\text{B3LYP/D95++(d,p): } \Delta E^\ddagger = 1.4549\Delta E + 0.8140 \\ (n = 9, r = 0.994, \text{sd} = 1.03) \quad (2)$$

The equations are obtained by linear regression and the data given in parentheses are the parameters associated with the fitting process, where n is the number of data point, r is the correlation coefficient, and sd is the standard deviation of fitting. A schematic representation of the correlations is presented in Figure 3. It indicates that the deviation for the pair **7/8** is somewhat large. If this point is excluded, the correlation for both equations is improved, cf. the standard deviation of eqs 1 and 2 is reduced to 0.54 and 0.65, respectively. Especially, for the pair **7/8**, the difference in reaction barrier (ΔE^\ddagger) is lower than that in reaction energy (ΔE), which differs markedly from the others. The absolute value of ΔE^\ddagger is larger than or essentially equals that of ΔE for other pairs, as shown in Table 1. In addition, comparing the results obtained by B3LYP/D95(d,p) and those by B3LYP/D95++(d,p), we found that the regioselectivity becomes more significant at the B3LYP/D95++(d,p) level, i.e. the absolute value of ΔE and ΔE^\ddagger become larger, for almost all pairs when the diffuse functions are augmented. Again, the ΔE and ΔE^\ddagger for the pair **7/8** are abrupt exceptions and another exception is the ΔE^\ddagger for **9/10**. Such anomalous behavior of the pair **7/8** may have been associated with their

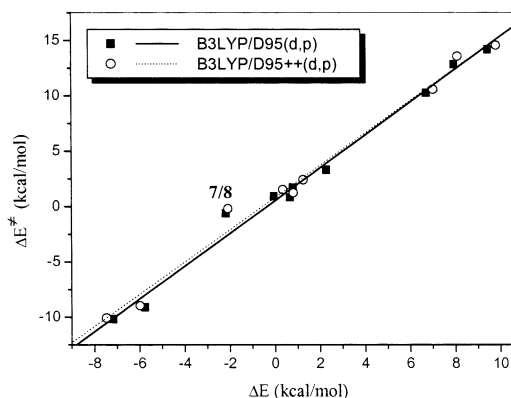


FIGURE 3. Correlations between calculated energy differences of carbinolamine intermediates and those of corresponding transition states at B3LYP/D95(d,p) and B3LYP/D95++(d,p) levels.

structural particularity. Part of structure of **7** is quite different from those of **5** and **9**, and part of **8** is quite different from those of **6** and **10**. Similarly, large differences are also found in the transition states. For example, the C_8-C_9 bond distance of **7** is shorter than that of **5** and **9** by 0.020 and 0.025 Å, respectively, while this bond distance of **7-TS** is shorter than that of **5-TS** and **9-TS** by 0.018 and 0.023 Å, respectively. The exocyclic C_8-N bond length of **8** is longer than that of **6** and **10** by 0.016 and 0.018 Å, respectively, while in the corresponding transition states, the values amount to 0.033 and 0.034 Å, respectively.

For the tricyclic model **11–16**, which consists of OBQ and two fused heterocyclic rings, we find that both the ΔE and ΔE^\ddagger are larger than those for bicyclic systems, predicting that these systems are more regioselective with respect to the condensation reaction. Moreover, both ΔE and ΔE^\ddagger are more than those of the adductive effect. For example, the ΔE for the pair **11/12** is 8.12 kcal/mol, larger than the sum of absolute value of the ΔE (6MIQ-I/7MIQ-I) and ΔE (**5/6**), $1.26 + 5.98 = 7.24$ kcal/mol; and the ΔE^\ddagger value of 13.17 kcal/mol is considerably larger than the sum of the value of ΔE^\ddagger (6MIQ-I/7MIQ-I) and ΔE^\ddagger (**5/6**), $8.97 + 2.42 = 11.39$ kcal/mol. This indicates that the electron-donating pyrrole and electron-withdrawing pyridine or pyrimidine have a somewhat synergistic effect on each other via medial structure. An examination of the geometries of **11–16** reveals that the dihedral angles $C_6-C_7-C_8-C_9$ for the carbinolamine intermediates with higher energy, **12**, **14**, and **16**, are obviously larger than those with lower energy, **11**, **13**, and **15**, respectively. The dihedral angles of the former set are all larger than 20° , while those of the latter set are all smaller than 2° . Therefore, the aforementioned argument that the carbinolamine intermediate with higher planarity possesses more thermodynamic stability is also suitable for these tricyclic model systems.

It is interesting to note that the condensation reactant of **15** or **16**, pyrrolo[2,3-*f*]quinoline-4,5-dione, represents the skeleton of PQQ. The reaction barrier, which is the difference between the transition state energy and the sum of the energies of pyrrolo[2,3-*f*]quinoline-4,5-dione and NH_3 , is calculated to be 21.44 kcal/mol at the B3LYP/D95(d,p) level if the tiny dipole-dipole complex is neglected, lower than that for MIQ, which is 32.70 kcal/

mol, and IIQ, 31.64 kcal/mol, by as much as 10.0 kcal/mol. Augmentation of diffuse functions in the calculation does not alter the results significantly, cf. the calculated barrier at the B3LYP/D95++(d,p) for the systems MIQ and the prototype PQQ is 32.92 and 21.82 kcal/mol, respectively. Therefore, it seems reasonable to deem that the larger catalytic effect of PQQ relative to TTQ at least partly results from the chemical characteristic of the ring structure itself.⁷ However, further investigation is expected since so far there have been no direct experimental data available for comparison.

Summary

The geometries of model compounds related to IIQ have been investigated at the B3LYP/D95(d,p) level. The optimized structure of IIQ is in good agreement with the experimental data. The differences in the part of geometries around the polar quinone group are slightly larger due to the occurrence of water near this area in the MADH crystal structure. The dihedral angle (χ) between the two indole rings of IIQ is optimized to be 49.6°. A scan of the potential energy surface along this dihedral angle shows that there is another local minimum with its energy higher than that of the global minimum by 0.74 kcal/mol. The transition state connecting the two minima has been located and found to be only 1.71 kcal/mol higher in energy than the global minima. Moreover, the PES scan shows the energetic difference is within 1.0 kcal/mol at a range of χ from 30° to 75°. Hence, the rotation of inter-indole rings is highly flexible. Vibrational frequency analysis reveals that IIQ is more delocalized compared to MIQ and OBQ.

The origin of regioselectivity for the condensation reactions of the models MIQ and IIQ with NH₃ has been elucidated. Population analysis of MIQ shows that the difference in the electronic structure between the two quinonoid carbons is ambiguous. However, energy calculations manifest that both the carbinolamine intermediate, which is the product of condensation reaction, and the corresponding transition state derived from nucleophilic attack at C-6 are preferentially formed,

consistent with the experimental observation. Therefore, the regioselectivity may well be ascribed to the energy differences of the two regioisomers and their corresponding transition structures. The substituted indole ring of IIQ can enhance the regioselectivity.

To investigate the effect of the fused ring on the regioselectivity of the condensation reaction, a series of models were designed. A good linear correlation has been found between the energy difference of the two different carbinolamine intermediates (ΔE) and that of the corresponding transition states (ΔE^\ddagger), suggesting that the factors stabilizing the carbinolamine intermediate also benefit the stability of the corresponding transition structure. In general, the carbinolamine intermediate keeping higher planarity is lower in energy and is preferentially formed during the condensation reaction. The couple **7/8** is an exception, which may be caused by their structural particularity. The tricyclic models, which consist of OBQ and two fused rings, are more regioselective. Moreover, the fused electron-donating pyrrole and the fused electron-withdrawing pyridine or pyrimidine exhibit a somewhat synergistic effect on each other via medial structure. The barrier of the condensation reaction for prototype PQQ described by model, **15**, is calculated to be ca. 22 kcal/mol. That is lower than the barrier for MIQ (ca. 33 kcal/mol) and IIQ (ca. 32 kcal/mol) by more than 10.0 kcal/mol, which seems to explain reasonably the larger catalytic effect of PQQ relative to TTQ.

Acknowledgment. This work was supported by the National Science Council of the Republic of China through Grant No. NSC 91-2113-M-007-034.

Supporting Information Available: The optimized geometries, vibrational frequencies scaled by 0.96, and natural population analysis at B3LYP/D95(d,p) for OBQ, MIQ, IIQ; several calculated structural parameters of IIQ scanned PES along the dihedral angle χ ; and optimized Cartesian coordinates and energies for all calculated structures. This material is available free of charge via the Internet at <http://pubs.acs.org>.

JO026793K